Journal of ELECTRONIC MATERIALS, Vol. 48, No. 3, 2019
https://doi.org/10.1007/s11664-018-06888-8

The Correlations between Complex Chemical Bond Theory and Microwave Dielectric Properties of $Ca_2MgSi_2O_7$ Ceramics

MI XIAO,[1,2] YANSHUANG WEI,[1] and PING ZHANG[1,3]

1.—School of Electrical and Information Engineering and Key Laboratory of Advanced Ceramics and Machining Technology of Ministry of Education, Tianjin University, Tianjin 300072, People's Republic of China. 2.—e-mail: xiaomi@tju.edu.cn. 3.—e-mail: zptai@163.com

Magnesium melilite ($Ca_2MgSi_2O_7$) ceramic with tetragonal crystal structure was prepared through the conventional solid-state method. Crystal structure and complex chemical bond theory were used to analyze the microwave properties of $Ca_2MgSi_2O_7$ ceramics and the correlations between the bond ionicity, lattice energy, bond energy and relative dielectric constant (ε_r), quality factor ($Q \times f_0$), temperature coefficient of resonant frequency (τ_f) were discussed in depth. Optimum microwave dielectric properties were obtained when sintered at 1300°C for 4 h: ε_r= 9.86, the dielectric loss (tanδ) was 1.24×10^{-4} (at 1 MHz), $Q \times f_0$= 8016 GHz (resonant frequency f_0 = 7.90 GHz), τ_f= − 42 ppm/°C.

Key words: $Ca_2MgSi_2O_7$, microwave dielectric properties, bond ionicity, lattice energy, bond energy

INTRODUCTION

With the development of microwave communication technology and radar system, the previous communication bands have been unable to meet the needs of modern communication. Microwave technology is developing towards higher frequency bands such as millimeter wave and submillimeter wave. In order to reduce the phenomenon of signal delay in millimeter wave bands, microwave materials used for the substrate of microwave circuits should have low dielectric constant and high quality factor.[1] Thus, the related research is attracting increasing attention.[2]

Low dielectric constant materials mainly include Al_2O_3, spinel structure ceramic systems and silicate ceramic systems.[3,4] Because of the tetrahedral structure [SiO_4] and the effects of the strong covalent bond, silicates present lower dielectric constant than others and have received much attention.[5] So far, many studies about silicate systems have been carried out. Kimata[6] reported the tetragonal crystal structure of $Ca_2CoSi_2O_7$. Next, Joseph et al.[7] reported that the $Sr_2ZnSi_2O_7$ ceramics had the same crystal structure as $Ca_2CoSi_2O_7$, and the sample doped with 2 wt.% $SrTiO_3$ showed good dielectric properties: $Q \times f_0$= 60000 GHz, ε_r= 8.8 and τ_f= −13 ppm/°C. $Ca_2MgSi_2O_7$ ceramic was usually doped with rare earth elements, such as Eu^{2+}, Ce^{3+} and Dy^{3+}[8–10] to study luminescent properties of materials. The sintering characteristics and dielectric properties of $Ca_2MgSi_2O_7$ were reported for the first time by Zhao and Wang[11] in 2014, and the ceramic presented good dielectric properties when sintered at 1280°C: relative dielectric constant (ε_r) was 7.6, the dielectric loss (tanδ) was 2.5×10^{-3}. However, quality factor ($Q \times f_0$) and the relationships between the complex chemical bond theory and the microwave dielectric properties have not been studied yet.

In this article, through changing the sintering process of $Ca_2MgSi_2O_7$ ceramics, the dielectric loss can be sharply reduced from 7.95×10^{-3} to 1.24×10^{-4}. Based on the chemical bond theory, the bond ionicity, lattice energy and bond energy were calculated and correlations with the microwave dielectric properties were further studied.

(Received August 23, 2018; accepted December 13, 2018; published online January 4, 2019)

EXPERIMENTAL PROCEDURE

The $Ca_2MgSi_2O_7$ ceramics were synthesized using conventional solid-state processing with highly analytical pure reagents of $CaCO_3$, MgO, SiO_2 as the starting materials. The materials were weighted based on the formula of $Ca_2MgSi_2O_7$ and then placed in nylon containers with ZrO_2 balls and distilled water and ball milled for 8 h. Then the obtained slurries were dried at 110°C, the powders were calcined at 1200°C for 4 h and ball milled again for another 6 h before drying. Next the powders were mixed with 15 wt.% paraffin as adhesive and sieved through a screen with 60 mesh. Finally, the powders were pressed into pellets 15 mm in diameter and 7.5 mm in thickness. During the sintering process, firstly, the temperature rose to 550°C at a heating rate of 5°C/min, then stayed at 550°C for a certain period of time, finally heating up to 1260–1320°C for 4 h in air at a heating rate of 5°C/min.

The phase of the sintered samples was identified by x-ray diffraction (XRD, Rigaku D/max 2550 PC, Tokyo, Japan) with Cu Kα radiation generated at 40 kV and 40 mA. The micro-morphologies of the ceramic surfaces were observed by scanning electron microscopy (SEM, MERLIN Compact, Germany). The dielectric loss was tested using a high-precision inductance capacitor resistance (LCR) meter (Agilent E4981A, USA) under a frequency of 1 MHz. The microwave dielectric properties of ceramics were measured by an HP8720ES network analyzer from frequency 5–15 GHz. The open cavity method was used to test the dielectric resonance frequency. The closed chamber method was used to measure the central frequency, loaded Q value and insertion loss in the $TE_{01\delta}$ mode, from which the dielectric constant ε_r and the unloaded Q value of the sample can be calculated. The temperature coefficients of resonant frequency (τ_f) were calculated according to the following equation:

$$\tau_f = \frac{f_2 - f_1}{f_1(T_2 - T_1)} \quad (1)$$

where f_1 and f_2 are the resonant frequency at T_1 (25°C) and T_2 (85°C), respectively.

The apparent densities ρ_{bulk} of the samples were calculated with Archimedes method (Mettler ToledoXS64). The theoretical density ρ_{theory} could be defined as follows:

$$\rho_{theory} = \frac{ZA}{V_C N_A} \quad (2)$$

where V_C, N_A, Z and A are volume of unit cell (cm^3), Avogadro constant (mol^{-1}), number of atoms in a unit cell, and atomic weight (g/mol), respectively. The relative density is defined as ratio of ρ_{bulk} to ρ_{theory}:

$$\rho_{relative} = \frac{\rho_{bulk}}{\rho_{theory}} \times 100\% \quad (3)$$

RESULTS AND DISCUSSION

Paraffin Removal Time and Relative Density Analysis

Measurement results of dielectric loss (tanδ) of samples sintered at 1300°C holding at 550°C for a certain period of time are shown in Fig. 1. When the temperature increases up to 550°C, paraffin is gradually removed from the green bodies in the form of paraffin vapor or the decomposition product CO_2 and holding at 550°C for a period of time to remove the paraffin more adequately. From Fig. 1, it can be seen that the holding time of paraffin removal at 550°C has a great influence on the dielectric properties of ceramics. When the holding time is too short, the decomposition product of CO_2 or paraffin molecules in the samples may not be fully removed, while after a long enough holding time at 550°C, the residual paraffin can be fully removed, causing the degree of densification of ceramics to increase during the following sintering process and making dielectric loss decrease sharply, which is consistent with the effect of paraffin removal on the properties of ceramics reported by Shan and Zhao.[12] It can be also found in Fig. 1 that the dielectric loss has little change with the further increase of holding time. So in the following study, the holding time at 550°C is all kept as 3 h.

The relative densities of the samples sintered at different temperatures are shown in Fig. 2. It was found that the relative density increased with the sintering temperature in the range of 1260–1300°C and reached a maximum value of 94.31% when the sintering temperature was 1300°C. However, when

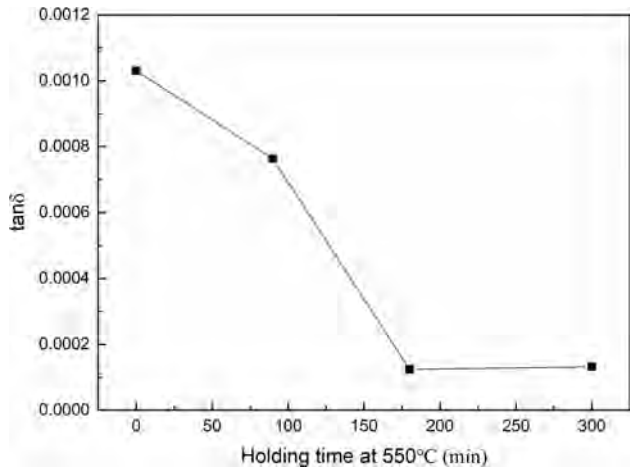

Fig. 1. The values of dielectric loss sintered at 1300°C holding at 550°C for 0 min, 90 min, 180 min and 300 min.

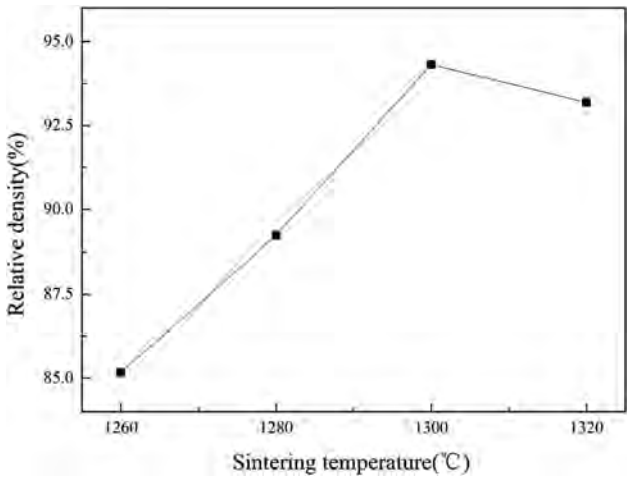

Fig. 2. The relative density of $Ca_2MgSi_2O_7$ ceramics sintered at 1260–1320°C.

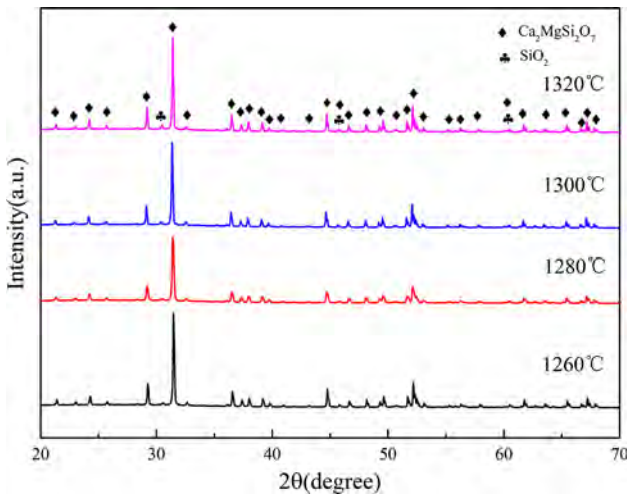

Fig. 3. The XRD patterns of $Ca_2MgSi_2O_7$ ceramics sintered at different sintering temperatures.

the sample was sintered at 1320°C, the relative density decreased. Through the sintering process, the grains gradually grew and the pores were gradually eliminated. As a result, with the decrease of surface energy, the relative density gradually increased. But when the sintering temperature was too high, the densification process became too fast, so many pores were enclosed in the grains, resulting in a decrease of densification.[13]

X-ray Diffraction Analysis

The x-ray diffraction patterns of $Ca_2MgSi_2O_7$ ceramics sintered at different temperatures are shown in Fig. 3. The main phase of tetragonal crystal structure with space group P-421m (113) could be confirmed, as well as a small amount of SiO_2 as a second phase. It could be also found that with the increase of sintering temperature, the intensity of SiO_2 diffraction peaks did not change obviously. And it had been confirmed that the appearance of second phase of SiO_2 was not oriented from the inaccuracy weighing of starting materials. This result was in accordance with the early report of Zhao and Wang.[11]

In this article, the Rietveld refinement of XRD patterns was performed using the software Fullprof. The reliable parameters of crystal structure could be obtained by importing the standard Crystallographic Information File (CIF) of a compound, and the background parameters, cell parameters, instrumental parameters, atomic parameters and shape parameters were refined to improve the accuracy of refinement. The reliability of the results was represented by the Rietveld discrepancy factors R_p and R_{wp}. The reliable lattice parameters could be obtained when R_p and R_{wp} were all lowered less than 15%,[14] The Rietveld refinement results were used to explain the effects of the sintering temperature on the $Ca_2MgSi_2O_7$ ceramics, and in this way the microwave dielectric properties could be analyzed based on the complex chemical bond theory. The obtained lattice parameters are listed in Table I.

Surface Morphology Analysis

The SEM photographs of $Ca_2MgSi_2O_7$ ceramics sintered at 1260–1320°C for 4 h are shown in Fig. 4. It can be seen from Fig. 4a that some pores appeared in the surface of the sample and the grains were small. When the sintering temperature increased from 1260°C to 1300°C, the pores gradually disappeared and the grains became larger. In particular, when sintered at 1300°C, the sample was more densified and smoother. However, when the sintering temperature exceeded 1300°C, the boundaries between grains were no longer obvious and over-heated phenomenon could be confirmed.

Crystal Structure Analysis

Magnesium melilite ($Ca_2MgSi_2O_7$) ceramic belongs to tetragonal structure ($\alpha = \beta = \gamma = 90°$, $a = b \neq c$) and the crystal structure is shown as Fig. 5. There are two molecules in the unit cell. The coordination number of Ca^{2+} is 8, and the coordination numbers of Mg^{2+}, Si^{4+} and O^{2-} are all 4.

The concept of chemical bonds in crystals has been widely used in chemistry and solid physics. Among them, the ionic description theory developed by Phillips and Van Vechten at the end of the 1960s has attracted great attention because it can be successfully applied to the calculation of bond structure, elastic and piezoelectric coefficients, valence bond parameters, and so on.[15,16] However, the object of this theory is only confined to A^NB^{8-N} type compound crystals. In 1973, Levine successfully extended the P–V theory to the A_mB_n-type crystals but failed to extend the theory to the complex crystal structures of multiple crystals due to some difficulties in models and methods.[17]

Table I. The lattice parameters and unit cell volume of $Ca_2MgSi_2O_7$ ceramics

T_S (°C)	a (Å)	b (Å)	c (Å)	$\alpha = \beta = \gamma$	V_{unit} (Å^3)	R_p (%)	R_{wp} (%)
1260	7.8419	7.8419	5.0147	90	308.38	13.41	9.72
1280	7.8454	7.8454	5.0161	90	308.74	12.31	8.35
1300	7.8509	7.8509	5.0200	90	309.42	11.96	7.44
1320	7.8449	7.8449	5.0159	90	308.69	12.73	9.23

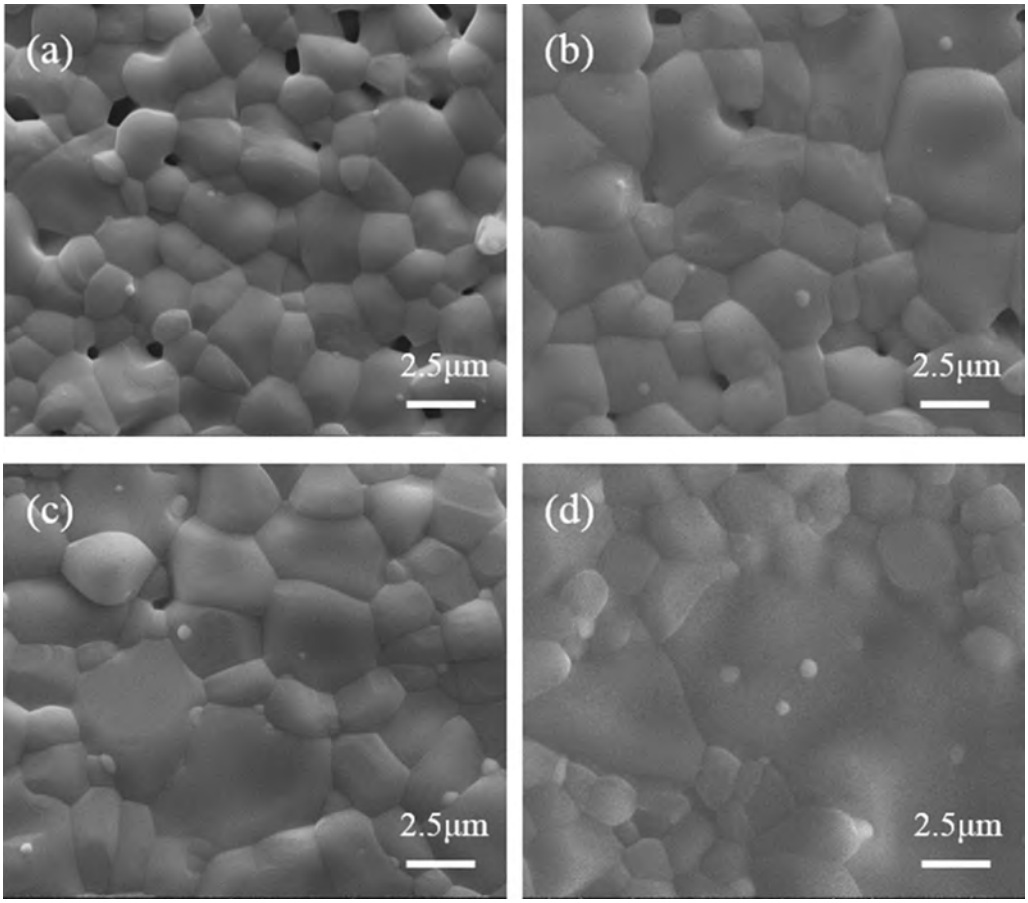

Fig. 4. SEM micrographs of $Ca_2MgSi_2O_7$ ceramics sintered at different sintering temperatures for 4 h: (a) 1260°C, (b) 1280°C, (c) 1300°C, (d) 1320°C.

Recently, Zhang and Zhao successfully generalized Phillips–Van Vechten–Levine theory for the analysis of multi-bond systems.[18]

In order to solve the problem of chemical bond calculation in complex crystals, the first task is to establish a method of decomposing the complex system of multiple types of chemical bonds into a single system of chemical bonds. The chemical molecular formula for any of the binary crystal corresponding to A–B chemical bonds can be written as follows:

$$\frac{N(B^j - A^i)a_i}{N_{CAi}} A^i \frac{N(A^i - B^j)b_j}{N_{CBj}} B^j \tag{4}$$

Thus, the molecular formula of any complex crystal can be written as the sum of binary crystals by the following equation:

$$A_{a1}^1 A_{a2}^2 \cdots A_{ai}^i B_{b1}^1 B_{b2}^2 \cdots B_{bj}^j = \sum_{i,j} A_{m_i}^i B_{n_j}^j \tag{5}$$

$$m_i = \frac{N(B^j - A^i)a_i}{N_{CAi}} \tag{6}$$

$$n_j = \frac{N(A^i - B^j)b_j}{N_{CBj}} \tag{7}$$

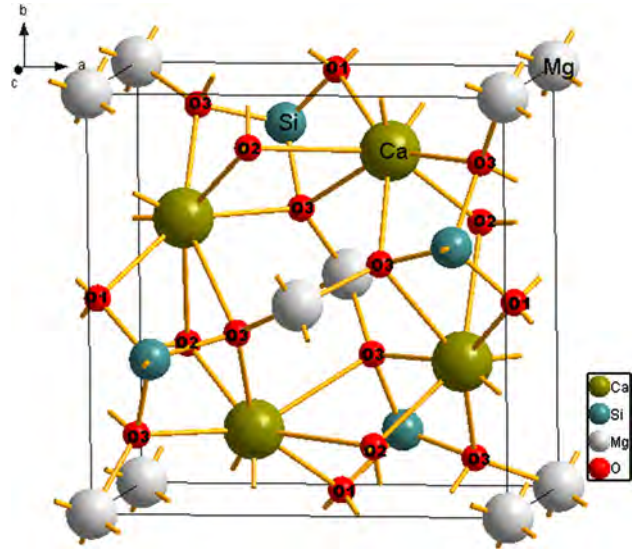

Fig. 5. Crystal structure of $Ca_2MgSi_2O_7$ ceramics.

where A and B represent the cation and the anion, A^i and B^j represent different symmetric sites of different elements or the same element, the numbers of the corresponding elements are a_i and b_j, respectively, the adjacent coordination numbers in the crystal are N_{cAi} and N_{cBj}, $N(I-J)$ indicates the number of I ions contained in the ligands of J ions.

Based on the crystal structure of $Ca_2MgSi_2O_7$ ceramics and Phillips–Van Vechten–Levine theory, the $Ca_2MgSi_2O_7$ could be split into the sum of binary crystals as follows:

$$\begin{aligned} Ca_2MgSi_2O_7 &= Ca_{1/4}O(1)_{1/2}+Ca_{3/4}O(2)_{3/2}+CaO(3)_2 \\ &\quad + MgO(3) + Si_{1/2}O(1)_{1/2}+Si_{1/2}O(2)_{1/2} \\ &\quad + SiO(3) \\ &= Ca_{1/4}O(1)_{1/2}+Ca_{1/2}O(2)^1+Ca_{1/4}O(2)^2_{1/2} \\ &\quad + Ca_{1/2}O(3)^1+Ca_{1/2}O(3)^2+MgO(3) \\ &\quad + Si_{1/2}O(1)_{1/2}+Si_{1/2}O(2)_{1/2}+SiO(3) \end{aligned}$$

In the $Ca_2MgSi_2O_7$ ceramic, the effective valence electron numbers Z are $Z_{Ca}= 2$, $Z_{Mg}= 2$, $Z_{Si}= 4$, and there are three types of bond (Ca–O, Mg–O, Si–O) for oxygen ions. The effective valence electron numbers of oxygen anions Zo are $Z_{Ca-O}= -1$, $Z_{Mg-O}= -2$, $Z_{Si-O}= -4$, respectively. The effective valence electron number of each ion is essential for the analysis of the lattice energy.

Microwave Dielectric Properties Analysis

Dielectric Constant Analysis

The dielectric constant shows the ability of polarization of dielectrics under an electric field. The polarization mechanisms in microwave dielectrics are mainly electron displacement polarization and ionic displacement polarization. So the dielectric constant has a strong relationship with ionic polarizabilities. In addition, the relative density and the second phase also show effects on the dielectric constant.[19,20] In this work, the dielectric constant of $Ca_2MgSi_2O_7$ ceramic system is mainly affected by the ionic polarizabilities because the pores gradually decrease and the amount of second phase is rather small. Since the ionic polarizability is proportionate to the bond ionicity, the bond ionicity can be used to analyze the change of dielectric constant.[21] The relationship between the bond ionicity f_i and dielectric constant ε_r is as follows:

$$\varepsilon_r = \frac{n^2-1}{1-f_i}+1 \tag{8}$$

where n represents the index of refraction.

Based on the generalized P–V–L theory, the bond ionicity f_i^μ and bond covalence f_c^μ of any type bond μ can be calculated as follows:

$$f_i^\mu = \frac{(C^\mu)^2}{(E_g^\mu)^2} \tag{9}$$

$$f_c^\mu = \frac{(E_h^\mu)^2}{(E_g^\mu)^2} \tag{10}$$

where the E_g^μ is the average energy interval and includes homopolar parts E_h^μ and heteropolar parts c^μ.

The calculation details of E_h^μ and C^μ can be referred to the Ref. 19 and the calculated results of the bond ionicity are shown in Table II.

From the data in Table II, it can be found that the value of the bond ionicity of the Ca–O bond, which is much higher than that of Mg–O and Si–O bonds, accounts for the main part in the total bond ionicity. So it has a dominant effect on the dielectric constant of $Ca_2MgSi_2O_7$ ceramics. The relationship between the average bond ionicity of Ca–O bond and relative dielectric constant is shown in Fig. 6. It can be seen that the changing trend of ε_r is consistent with that of bond ionicity, which coincides with the description of Eq. 8. Powder particles have high surface energy. According to the lowest energy principle, the particle will change spontaneously to the lowest energy state. The ionic bond is a stable chemical bond formed by the energy of the whole system to the lowest point. When the sintering temperature rises, the bond length changes, and then the bond ionicity increase, which causes the dielectric constant to increase.

Quality Factor Analysis

The quality factor of microwave dielectric ceramics can be affected by extrinsic losses and intrinsic losses. The extrinsic losses are mainly affected by grain size, porosity and second phases while the

Table II. Bond ionicity f_i (%) of $Ca_2MgSi_2O_7$ ceramics

Bond ionicity f_i (%)	1260°C	1280°C	1300°C	1320°C
Ca–O(1)	90.5731	90.6167	90.5670	90.5835
Ca–O(2)[1]	90.2591	90.2686	90.2595	90.3017
Ca–O(2)[2]	91.0349	91.0090	91.0100	90.9872
Ca–O(3)[1]	91.0753	91.0884	91.1073	91.1151
Ca–O(3)[2]	90.2328	90.1980	90.2711	90.2583
Mg–O(3)	59.3946	59.6904	59.4158	59.5706
Si–O(1)	75.7207	75.9737	75.5430	75.6445
Si–O(2)	76.5504	76.4609	76.6211	76.7292
Si–O(3)	76.7251	76.4749	76.4355	76.4346
$Af_{iCa–O}$	90.6350	90.6361	90.6430	90.6492

$A_{fiCa–O}$ is the average bond ionicity of Ca–O bond.

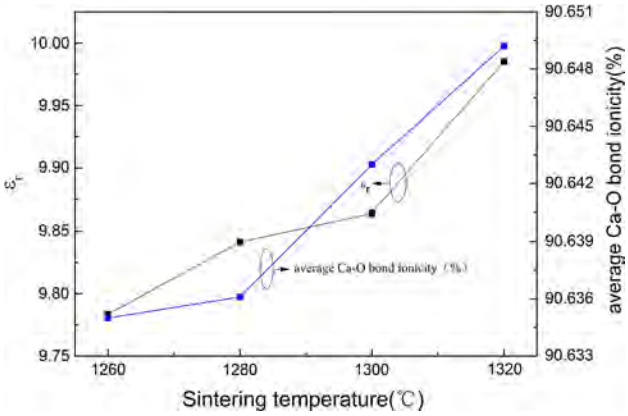

Fig. 6. Dielectric constant and the average Ca-O bond ionicity of $Ca_2MgSi_2O_7$ ceramics.

Table III. Lattice energy U (kJ mol^{-1}) of $Ca_2MgSi_2O_7$ ceramics

Bond type	1260°C	1280°C	1300°C	1320°C
Ca–O(1)	656	653	655	655
Ca–O(2)[1]	682	682	681	679
Ca–O(2)[2]	1229	1234	1231	1239
Ca–O(3)[1]	1220	1219	1212	1214
Ca–O(3)[2]	1368	1374	1360	1365
Mg–O(3)	4199	4154	4191	4174
Si–O(1)	8976	8868	9041	9016
Si–O(2)	8593	8640	8545	8512
Si–O(3)	17,011	17,268	17,273	17,317
$AU_{Si–O}$	11,527	11,592	11,620	11,615

$AU_{Si–O}$ is the average Si–O lattice energy.

intrinsic loss is mainly dominated by lattice anharmonicity.[22] Zhang et al.[23] had reported that the quality factor had a close relationship with the lattice energy of samples. The calculation method of lattice energy U_{cal} of complex crystal is as follows:

$$U_{cal} = \sum_{\mu} U_b^{\mu} \tag{11}$$

$$U_b^{\mu} = U_{bc}^{\mu} + U_{bi}^{\mu} \tag{12}$$

$$U_{bc}^{\mu} = 2100\,\mathrm{m}\,\frac{(Z_+^{\mu})^{1.64}}{(d^{\mu})^{0.75}} f_c^{\mu} \tag{13}$$

$$U_{bi}^{\mu} = 1270\,\frac{(m+n)Z_+^{\mu}Z_-^{\mu}}{d^{\mu}}\left(1 - \frac{0.4}{d^{\mu}}\right) f_i^{\mu} \tag{14}$$

where U_{bc}^{μ} and U_{bi}^{μ} are ionic energy and covalent energy, respectively, f_i^{μ} and f_c^{μ} are ionic and covalent parts, Z_+^{μ} and Z_-^{μ} are the valence states of cations and anions presented in μ bond valence, respectively; m^{μ} and n^{μ} are the numbers of cations and anions of any μ bond; d^{μ} is the bond length of the μ bond.

The calculation results of the lattice energy of $Ca_2MgSi_2O_7$ ceramics are shown in Table III. The tanδ values (tested at 1 MHz) of $Ca_2MgSi_2O_7$ ceramics at different sintering temperature and the correlation between the quality factor and the average Si–O lattice energy are shown in Fig. 7a and b, respectively. It can be found in Fig. 7a that the tanδ value reduced from 7.95×10^{-3} to 1.24×10^{-4} when the sintering temperature increased from 1260°C to 1300°C. When sintered at 1320°C, the tanδ value is a bit increased to 1.53×10^{-4}. From Fig. 7b we can find that $Q \times f_0$ increases first and then decreases at 1320°C. The decrease of tanδ and increase of $Q \times f_0$ values is related to the reduction of porosity and the gradual growth of grains according to the results of SEM photographs in Fig. 4a, b, and c. Because of the over-heating phenomenon, as shown in Fig. 4d, the $Q \times f_0$ values decreased. These are extrinsic factors. From Fig. 7b we can also find that the variation of

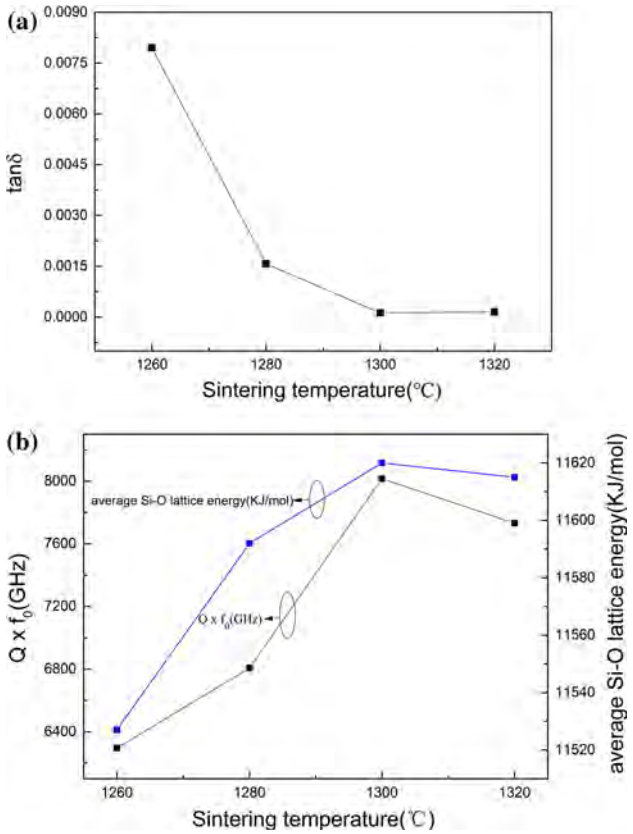

Fig. 7. (a) The tanδ values of $Ca_2MgSi_2O_7$ ceramics sintered at 1260–1300°C, (b) $Q \times f_0$ and the average Si–O lattice energy of $Ca_2MgSi_2O_7$ ceramics.

Table IV. Bond energy E (kJ mol^{-1}) of $Ca_2MgSi_2O_7$ ceramics

Bond type	1260°C	1280°C	1300°C	1320°C
Ca–O(1)	276.0039	274.2529	275.7838	275.8938
Ca–O(2)^1	289.3999	289.1580	288.9164	287.9541
Ca–O(2)^2	254.8511	256.2675	255.5101	257.5078
Ca–O(3)^1	252.8943	252.4328	250.7853	251.3321
Ca–O(3)^2	290.4939	292.0886	288.4345	289.7637
Mg–O(3)	315.8632	311.2035	315.0209	313.3497
Si–O(1)	551.6606	541.4698	557.9613	555.4940
Si–O(2)	516.3517	520.6317	512.1415	509.1760
Si–O(3)	508.5870	520.0159	520.3237	522.1775
AE_{Si-O}	525.5331	527.3725	530.1422	528.9492

AE_{Si-O} is the average Si–O bond energy.

$Q \times f_0$ is consistent with the Si–O lattice energy. So in the case of $Ca_2MgSi_2O_7$ in our experiments, both extrinsic and intrinsic factors took effects. Because of the Si–O lattice energy value is higher than that of Ca–O, Mg–O bond, the U_{Si-O} take predominant contribution to the $Q \times f_0$ value. The largest $Q \times f_0$ value of 8016 GHz is obtained when the sintering temperature is 1300°C.

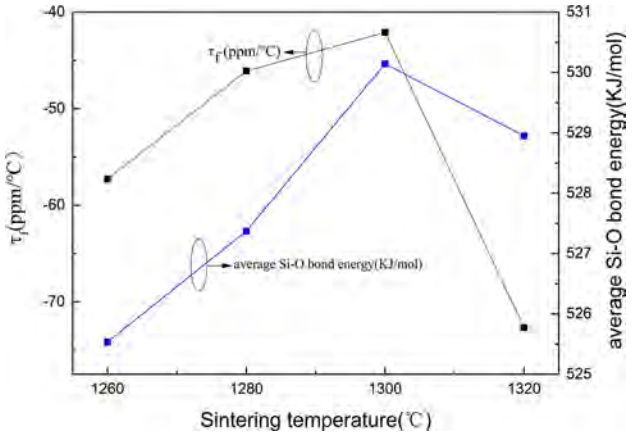

Fig. 8. τ_f and the average Si–O bond energy of $Ca_2MgSi_2O_7$ ceramics.

Temperature Coefficient of Resonant Frequency Analysis

Temperature coefficient of resonant frequency is in connection with the lattice stability, the more stable the lattice, the smaller the temperature coefficient. The stability of the lattice is related to the value of the bond energy, greater bond energy can stabilize the vibration of the ions in the lattice. Xiao et al. reported that the bond energy could affect the temperature coefficient of resonant frequency by affecting bond length.[12] The greater the bond energy, the smaller the value of $|\tau_f|$.

Based on the electronegativity and bond energy theory,[24] the bond energy can be defined as follows:

$$E = \sum_{\mu} E_b^{\mu} \tag{15}$$

$$E_b^{\mu} = t_c E_c^{\mu} + t_i E_i^{\mu} \tag{16}$$

$$E_i^{\mu} = \frac{33200}{d^{\mu}} \tag{17}$$

$$E_c^{\mu} = \frac{(r_{CA} + r_{CB})}{d^{\mu}} (E_{A-A} + E_{B-B})^{\frac{1}{2}} \tag{18}$$

$$t_i + t_c = 1 \tag{19}$$

where E_b^{μ} is bond energy and includes nonpolar covalence energy E_c^{μ} and complete ionicity energy E_i^{μ}; r_{cA} and r_{cB} represent covalent radii, E_{A-A} and E_{B-B} are the homonuclear bond energy that can be obtained from the handbook,[25] t_i and t_c are the ionic and covalent blending coefficients, respectively. In this work, E_{Ca-Ca} = 16.8 kJ mol^{-1}, E_{Mg-Mg} = 11.3 kJ mol^{-1}, E_{Si-Si} = 310 kJ mol^{-1}, E_{O-O} = 498.36 kJ mol^{-1}.

The calculation results of bond energy of $Ca_2MgSi_2O_7$ ceramics are shown in Table IV. From the

listed data, we can see that with the increase of sintering temperature, the average Si–O bond energy increased firstly and then decreased at 1320°C, which indicated that the system was more stable at the sintering temperature of 1300°C. The changing trend of τ_f and average Si–O bond energy with different sintering temperatures are shown in Fig. 8. The variation trend was coincident with that of average Si–O bond energy. When sintered at 1300°C, the absolute value of τ_f is the smallest, which is − 42 ppm/°C.

CONCLUSION

In this work, the dielectric properties of $Ca_2MgSi_2O_7$ ceramics were studied. It was proved that the pure single-phase of $Ca_2MgSi_2O_7$ ceramics was difficult to obtain due to the existence of second phase SiO_2. The study of effects of different paraffin removal holding time on dielectric loss proved that appropriate holding time at 550°C could make dielectric loss smaller. The open cavity and closed chamber method were used to measure microwave dielectric properties. The relationships among the bond ionicity, lattice energy and bond energy and microwave dielectric properties were discussed. With the increase of sintering temperature, the bond ionicity all increased, the lattice energy and the bond energy increased firstly and reached the maximum value at 1300°C, then decreased. The changing trends of relative dielectric constant and temperature coefficient of resonant frequency were coincident with the bond ionicity and bond energy, respectively. The quality factor was affected by the lattice energy of Si–O bond as intrinsic factors. In addition, it was also influenced by extrinsic losses. $Ca_2MgSi_2O_7$ ceramics sintered at 1300°C for 4 h showed excellent microwave dielectric properties: ε_r= 9.86, $\tan\delta = 1.24 \times 10^{-4}$ (at 1 MHz), $Q \times f_0$= 8016 GHz (resonant frequency f_0 = 7.90 GHz), τ_f= − 42 ppm/°C, making it fit for the production of microwave substrate and relative applications.

ACKNOWLEDGMENTS

This work was supported by the National Natural Science Foundation of China (No. 61671323).

REFERENCES

1. M.M. Krzmanc, M. Valant, and D. Suvorov, *J. Eur. Ceram. Soc.* 27, 1181 (2007).
2. P. Zhang, J. Liao, Y. Zhao, H. Xie, L. Liu, and M. Xiao, *J. Mater. Sci.: Mater. Electron.* 28, 4946 (2017).
3. H. Wang, Q. Zhang, H. Yang, and H. Sun, *Ceram. Int.* 34, 1405 (2008).
4. M.E. Song, J.S. Kim, M.R. Joung, S. Nahm, and Y.S. Kim, *J. Am. Ceram. Soc.* 91, 2747 (2010).
5. H. Ohsato, T. Tsunooka, T. Sugiyama, K.I. Kakimoto, and H. Ogawa, *J. Electroceram.* 17, 445 (2006).
6. M. Kimata, *NW* 69, 40 (1982).
7. T. Joseph and M.T. Sebastian, *J. Am. Ceram. Soc.* 93, 147 (2010).
8. C. Xu, J. Guo, Y. Li, and H.J. Seo, *Opt. Mater.* 35, 893 (2013).
9. I.P. Sahu, *J. Mater. Sci.: Mater. Electron.* 27, 9094 (2016).
10. I.P. Sahu, D.P. Bisen, R.K. Tamrakar, and R. Shrivastava, *Res. Chem. Intermed.* 42, 1823 (2016).
11. X.H. Zhao, M.J. Wang, Q.L. Zhang, H. Yang, L. Hu, and D. Yu, *Mater. Lett.* 122, 9 (2014).
12. L.J. Shan and L.X. Zhao, *Ceramics* 2, 7 (2007).
13. M. Xiao, J. Lou, Y. Wei, and P. Zhang, *Ceram. Int.* 44, 885 (2018).
14. M. Xiao, J. Lou, and Z. Zhou, *Ceram. Int.* 43, 15567 (2017).
15. J.C. Phillips, *Phys. Rev. Lett.* 20, 550 (1968).
16. J.C. Phillips and J.A. Van Vechten, *Phys. Rev. Lett.* 22, 705 (1969).
17. B.F. Levine, *J. Chem. Phys.* 59, 1463 (1973).
18. Z.J. Wu, Q.B. Meng, and S.Y. Zhang, *Phys. Rev. B* 58, 958 (1998).
19. E.S. Kim and K.H. Yoon, *J. Eur. Ceram. Soc.* 23, 2397 (2003).
20. R.D. Shannon, *J. Appl. Phys.* 73, 348 (1993).
21. P. Zhang, Y. Zhao, and X. Wang, *Dalton Trans.* 44, 10932 (2015).
22. J. Petzelt, J. Schwarzbach, and B.P. Gorshunnov, *Ferroelectrics* 93, 77 (1989).
23. P. Zhang, Y. Zhao, and L. Li, *Phys. Chem. Chem. Phys.* 17, 16692 (2015).
24. R.T. Sanderson, *J. Am. Chem. Soc.* 105, 2259 (1983).
25. Y.R. Luo, *Comprehensive Handbook of Chemical Bond Energies* (Boca Raton: CRC Press, 2007).